energies

MDPI

Article

Hybrid Switched Reluctance Motors for Electric Vehicle Applications with High Torque Capability without Permanent Magnet

Vijina Abhijith [1,*], M. J. Hossain [1,*], Gang Lei [1], Premlal Ajikumar Sreelekha [2,*], Tibinmon Pulimoottil Monichan [2] and Sree Venkateswara Rao [3]

[1] School of Electrical and Data Engineering, University of Technology Sydney, Ultimo, NSW 2007, Australia
[2] Entuple E-Mobility, Diamond District, HAL Old Airport Road, Kodihalli, Bangaluru 560008, India
[3] Gyrate the Motor Inside, Shimla Block, Hill country, Bachupallay, Telangana 500090, India
* Correspondence: vijina.abhijith@student.uts.edu.au (V.A.); jahangir.hossain@uts.edu.au (M.J.H.); premlal95111@gmail.com (P.A.S.)

Abstract: In electric vehicle (EV) applications, hybrid excitation of switched reluctance motors (HESRMs) are gaining popularity due to their advantages over other EV motors. The benefits include control flexibility, simple construction, high torque/power density, and the ability to operate over a broad speed range. However, modern HESRMs are constructed by increasing the air gap flux density with permanent magnets (PMs) in the excitation system in order to generate more electromagnetic torque. This study aims to investigate a new topology for increasing the torque capabilities of HESRM without the use of permanent magnets (PMs) or other rare-earth components. This paper provides a comprehensive evaluation of the static and dynamic characteristics, software analysis using the Ansys 2D finite element method (FEM), and an experimental demonstration of the real-time motor with an advanced control strategy in MATLAB/Simulink. Our simulation and experimental results for a machine with 12/8 poles and a machine rating of 1.2 kW indicate that the HESRM designed without PMs has greater torque capability and efficiency than the conventional SRM. The proposed HESRM without PMs has a high torque/power density and a higher torque per ampere across the entire speed range, making it suitable for EV applications.

Keywords: switched reluctance motor (SRMs); hybrid excitation of SRM (HESRM); hybrid excitation of SRM without a permanent magnet; permanent magnet (PM); electric vehicle motor

Citation: Abhijith, V.; Hossain, M.J.; Lei, G.; Sreelekha, P.A.; Monichan, T.P.; Rao, S.V. Hybrid Switched Reluctance Motors for Electric Vehicle Applications with High Torque Capability without Permanent Magnet. *Energies* **2022**, *15*, 7931. https://doi.org/10.3390/en15217931

Academic Editors: Vladimir Prakht, Mohamed N. Ibrahim and Vadim Kazakbaev

Received: 24 September 2022
Accepted: 21 October 2022
Published: 26 October 2022

1. Introduction

The widespread use of ICE (internal combustion engine) automobiles has led to an increase in pollution and energy constraints in recent years. The use of electric vehicles (EVs) has the potential to reduce environmental stress, reduce pollution, and limit the number of vehicles requiring charging [1]. Electric vehicles (EVs) rely heavily on electric motors [2]; thus, numerous electric motors were evaluated and analyzed to determine which would be the most effective for various applications. These days, brushless DC motors (BLDCMs), induction motors, and different permanent magnet (PM) machines are some of the motor types other than SRM motors that can be used effectively in variable-speed applications [3,4]. In comparison with conventional motors, SRMs are appealing to researchers due to their low complexity, high durability, cost-effectiveness, and ease of production [5,6]. SRM appears to have the same power density as induction motors, and its reliability appears to be far superior to that of DC series and permanent magnet motors [7]. As the SRM lacks the mechanical components of other conventional motors, such as permanent magnets and rotor windings, it can be utilized in high-temperature environments [8]. Low torque and power density, compared with permanent magnet motors, as well as significant torque ripple, are two drawbacks that limit its utility [9].

Numerous researchers are devoted to reducing the machine architecture to the level required by applications in order to address these problems and boost the performance of SRMs. Prior research has demonstrated that numerous approaches to switched reluctance motors focus on innovative controller circuits [10–12], core segmentation [13–16], and hybrid excitations (HESRMs).

Using sophisticated controller circuits, the switching circuit of the stator of an SRM can be optimized to provide maximum torque. Precision phase-winding switching makes it possible to tailor the performance of modern electronic converters to specific applications [17]. This accurate switching method permits substantial control over the torque ripple of the motor. In order to increase the available flux in the air gap and the resulting flux, the segmentation method [18] is applied to either the stator or rotor cores. By limiting the flux to the separated regions, the average torque of the active region is increased. This segmented system diminishes mechanical strength and contributes to higher costs [19] due to the increased production complexity. Due to the internal flux's reciprocal coupling, the overall efficiency of the segmented core is diminished. Drive circuits with multiple stator segments may be used for low- and high-speed applications and provide more power and torque per ampere [20]. This technique increases torque output at the expense of machine durability [21]. The third option (HESRM) is permanent magnet hybrid-excited switched reluctance motors.

SRMs underwent a paradigm shift with the introduction of the hybrid excitation technique, which substantially increased their ability to generate electromagnetic torque. However, this approach uses PMs into the structure of the machine to increase the motor's average torque. A 12/8 HESRM with a modular stator was presented in a stator segmented with PMs [22]. There is evidence that it can transport a maximum flux density at a higher torque [23]. The flux capacity is increased by 34.7% compared with the segmented SRM without PM [24]. As a result, the average torque is 71.4% greater than the conventional SRM. A comparison study of a segmented stator permanent magnet hybrid excitation SRM drive [25] reported that the static average torque of the segmented HESRM is 1.16 to 1.39 times that of the standard one. There were six permanent magnets (PMs) in the stator of the machine; due to the behavior of the PMs, this could cause cogging torque. It has been demonstrated that SRM with auxiliary winding and permanent magnets is 3% more efficient and reduces size and weight by the same amount [26]. The HESRM, meanwhile, combines the benefits of the permanent magnet machine and the electromagnet machine to create a hybrid excitation of the double salient machine [27]. The rare-earth permanent magnets in the rotor core of the 6-slot 8-pole hybrid excitation flux switching machine (HEFSM) are an innovative design element that contributes to the machine's high power density by providing adequate mechanical strength with enhanced electromagnetic performances [28]. The suggested machine, the HEFSM, has an efficiency ranging from 92 to 97 percent, and it is also used to dampen vibration and acoustic noise. Similar to low-power, low-cost applications, single-phase hybrid SRMs are utilized for low-power, low-cost applications. The new low-cost hybrid SRM for variable-speed pumps contains permanent magnets in the shape of rectangular shards. As a result, both the average torque and the torque ripple are increased; see [29].

However, the hybrid excitation method improves the efficiency of SRM due to the strategic placement of PMs. The PM's actions have the potential to deceive the SRM because they alter the SRM's typical behavior. Additionally, rare-earth metals and PMs are becoming increasingly scarce. In the era of electric automobiles, both cost-effective and efficient motors will be crucial. Nonetheless, the high demand and limited supply of PMs will increase the cost of manufacturing PM-equipped machines. To maintain a high torque/power density under these conditions, the PM's electric motor integration strategy is not a viable option. Therefore, this work primarily contributes to eliminating the need for permanent magnets in SRMs, while simultaneously enhancing torque performance via hybrid excitation techniques.

Due to the combined action of the two controllers, the proposed HESRM motor has better control over the motor. Because separate controllers are used for the main and auxiliary windings, it has more flexibility. The torque per ampere is improved by the proposed method because it produces more torque at lower current levels than the traditional SRM. The auxiliary windings can work at current control, while the main windings can work in speed control. To increase torque, auxiliary windings can be used to inject DC, and thus maximize the machine's potential. There is less redundancy because the motor is switched by two separate controllers, one of which can continue to operate the machine even if the other fails. This machine exhibits a significantly higher flux in its stator yoke than conventional machines, which is primarily caused by flux saturation in the core.

The remainder of this paper is organized as follows: Section 2 provides a detailed description of the proposed HESRM's machine topology and fundamental operations. In Section 3, the simulation results of the proposed machine's static and dynamic behavior, including the results of the machine's flux distribution, phase flux linkage, electromagnetic torque, etc., are described in detail. Furthermore, Section 4 discusses the construction of machines with identical dimensions and experimental validation. In Section 5, the average torques of HESRM are compared with those of a conventional SRM. Finally, Sections 6 and 7 cover the discussion and conclusion in detail.

2. Machine Topology for the Proposed Machine

The machine topologies of conventional SRM and the proposed HESRM without PMs are shown in Figure 1. Both motors have twelve stator and eight rotor poles without any PMs incorporated within the cores. Still, the windings of poles per phase are assigned for different excitation—main pole windings and auxiliary winding excitations, respectively, for the assigned poles. The new hybrid excitation technique's main goal is to boost the conventional SRM's torque performance without sacrificing any of its distinctive characteristics. Permanent magnets and structural changes are entirely avoided in HESRM. The excitation of the conventional SRM differs in that the windings are excited and separated separately to inject more external current into the HESRM. These auxiliary windings are selected so that two windings from each phase are separated, maintaining the motor's mechanical and electrical symmetry. Figure 1 depicts these alternately positioned auxiliary windings, which inject external DC current in accordance with the torque required by the controller. The motors' measured speed is sensed and fed back to create PWMs, which are then delivered to the throttle.

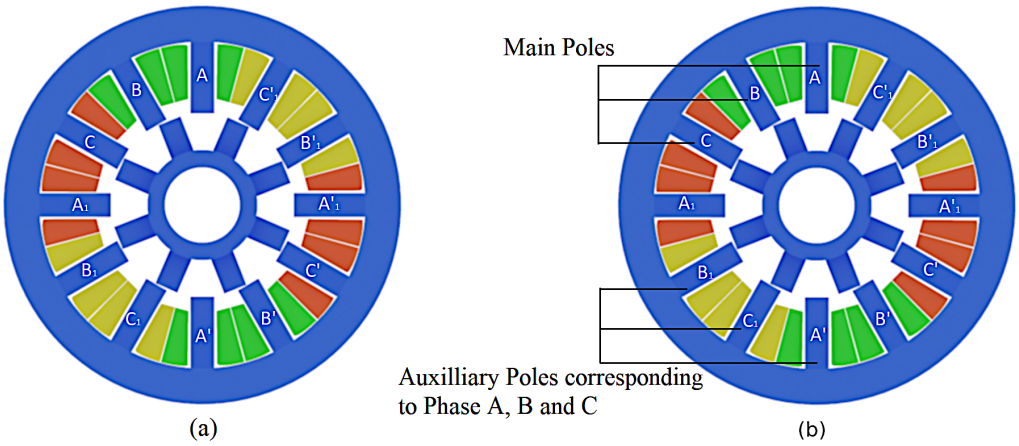

Figure 1. Machine topologies of two SRMs with the same rating as shown as (**a**) 12/8-pole conventional SRM and (**b**) 12/8-pole HESRM without PMs.

First, the poles are assigned for auxiliary excitation. The stator of the HESRM differs from that of the conventional SRM; in the HESRM, the stator poles are assigned to the main and auxiliary poles based on the excitation. Since there are twelve stator poles in the motor, six poles can be used for the primary excitation, while the remaining poles can be used for

the auxiliary excitation to provide the same three phases as conventional SRMs. Second, the number of poles for the primary and auxiliary windings is maintained constant in order to inject external flux into the poles simultaneously with the excitation of the primary windings. Separate DC excitation can increase the resultant flux in the air gap due to the symmetrical nature of the poles. Using electrical and mechanical symmetry, the primary and secondary poles are differentiated. This geometry of twelve stators can be utilized effectively to provide two distinct windings for each phase [30]. There are two distinct windings in HESRM: the main windings and the auxiliary windings. With the aid of a separately excited driver circuit, the auxiliary windings' poles inject DC current. The main windings provide the current for excitation of the motor. Because the variations in both windings' currents affect the air-gap flux density, the flux in HESRM is more than the traditional SRM. The new topology has a greater flux density, power, and torque without using the PM behavior.

Figure 2 is a structural diagram of magnetic field distribution that illustrates the fundamental operating principle of the proposed HESRM without PMs. It shows the magnetic field distribution of two SRMs with aligned and misaligned poles. Regardless of whether the SRMs are operating in an aligned or unaligned position, identical field lines can be observed. The HESRM flux is injected along the same path as the carryover path for the primary winding flux. Therefore, the flux due to auxiliary excitation can carry a greater flux to generate a greater electromagnetic torque. A detailed block diagram of the HESRM is shown in Figure 3. The new hybrid excitation technique's main goal is to boost the conventional SRM's torque performance without sacrificing any of its distinctive characteristics. Permanent magnets and structural changes are entirely avoided in HESRM. The excitation of the conventional SRM differs in that the windings are excited and separated separately to inject more external current into the HESRM. These auxiliary windings are selected so that two windings from each phase are separated, maintaining the motor's mechanical and electrical symmetry.

The net flux generated by HESRM in the absence of PMs travels through the core and then the air gap, creating a closed path similar to the conventional flux path. When both coils are excited, the flux intensity generated by the primary and secondary differs because the secondary pole can carry a greater current than the primary. The total flux produced by the primary coil and the auxiliary coils can be observed to be added. Consequently, the total magnetic flux produced by the HESRM is greater than the conventional flux without PMs. Consequently, the electromagnetic torque results from the algebraic sum of the total effective flux of both windings.

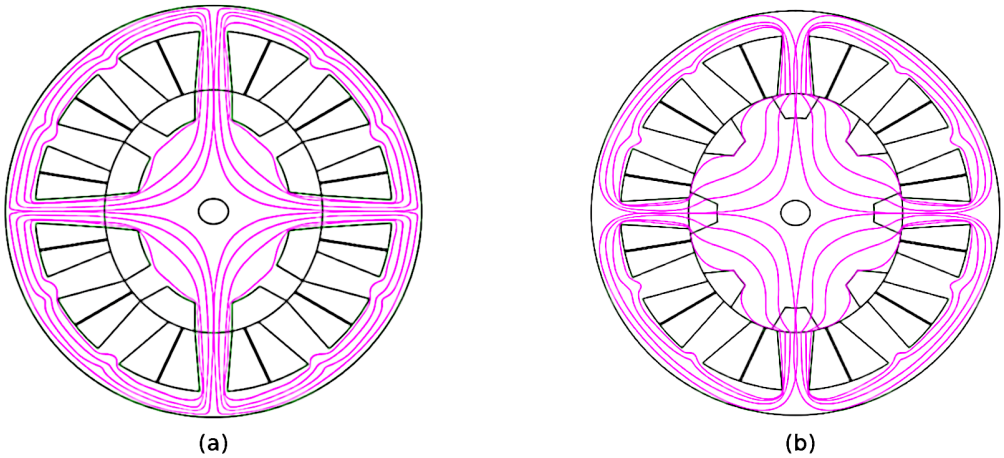

Figure 2. Magnetic field distributions of two SRMs with 12/8 poles s shown as: (**a**) aligned pole and (**b**) unaligned pole.

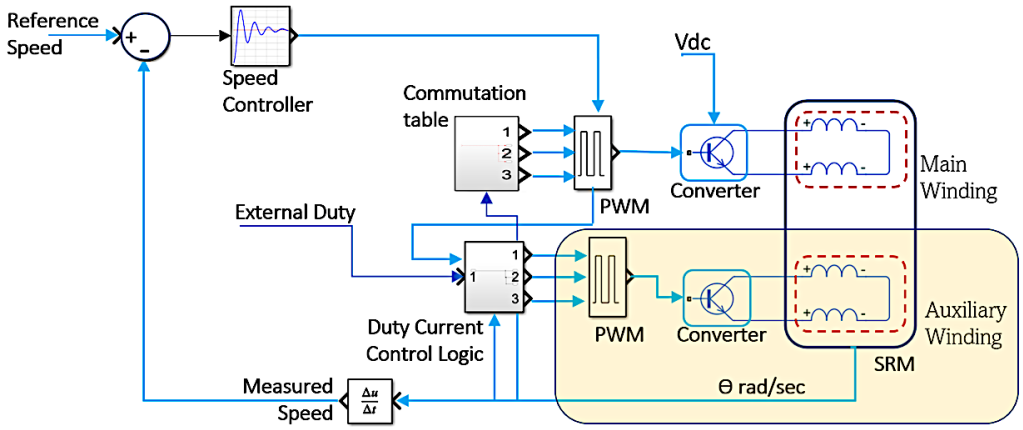

Figure 3. Block diagram of the proposed HESRM without permanent magnet excitation.

The dimensions and specifications of the conventional SRM and the proposed HESRM are listed in Table 1. Similarly, the number of phases, number of poles in the stator and rotor, rated power, speed, length of the core, and type of material are all identical. In addition, the assignment of the HESRM's auxiliary and primary poles differs based on the flux path.

Table 1. Main dimensions and parameters of two SRMs.

Dimensions	Conventional SRM	HESRM
Phase number	3	3
Stator and rotor poles	12/8	12/8
Hybrid excitation poles	12	6-6
Rated Power(kW)	1.2	1.2
Rated speed (rpm)	2500	2500
Outer dia of stator (mm)	138	138
Inner dia of rotor (mm)	81.50	81.50
Length of air gap (mm)	0.5	0.5
Type of material	M15_26G	M15_26G

3. Characteristics of the Proposed HESRM Using 2D FEA Analysis

This section presents the magnetic characteristics of the conventional SRM at aligned and unaligned positions. To obtain better clarity and easiness of comparison, both the SRMs are given the same size, number of coils per pole, and similar types of windings, as shown in Table 1. The field lines where the stator and rotor iron have the shortest flux path are concentrated in the aligned position rather than the unaligned one.

3.1. Magnetic Characteristics of Two SRM's

The cross-sectional areas of the two SRMs are the same due to the same rotor construction and geometric dimensions. Thus, both SRMs, the stators, and rotor iron weights identical to the constructions have a 7.933 (kg) total net weight, and the stator and rotor core steel consumptions (kg) are 7.05683 and 2.6735, respectively. Owing to the difference, only the excitation scheme provided the winding with different currents.

Field Line and Flux Distributions

The magnetic characteristics of the proposed SRM are similar to that of the conventional SRM. Here, the quantity of the flux lines will increase as more current is injected into the auxiliary poles. As a result, the effective flux lines in the air gap increase, and the resultant electromagnetic torque increases. Figures 4 and 5 demonstrate the magnetic flux distribution and the flux density of the conventional SRM and the proposed HESRM, respectively. The excitation for the three-phase scheme for the conventional SRM with

aligned and unaligned poles shows that the minimum flux density is 1.2–1.3 Tesla (T) for the unaligned pole and 1.7–1.8 T for aligned poles. The conventional SRM's range for maximum flux density is 0–1.9 T, and steel is the material used for the simulation. Figure 6 shows the conventional SRM for the given excitation (5A) at aligned and unaligned positions. At aligned position, it is 1.2 T, and at unaligned position, it is 1.6 T. Because the auxiliary windings' unexcited pole is aligned with the excitation pole in the HESRM, it can reach 1.06 T in alignment with the same excitation current (5A). Auxiliary injection current helps to increase the magnetic flux density in an unaligned state in 1.3 T, comparing the magnetic flux distribution and flux intensity of the proposed HESRM, where both characteristics are identical. Accordingly, there is only one difference in the intensity of flux carrying in the air gap due to different DC injections in the auxiliary poles. First, the excited state produces the main flux with the effect of the main winding, and the extra DC provided by the auxiliary excitation creates more electromagnetic torque.

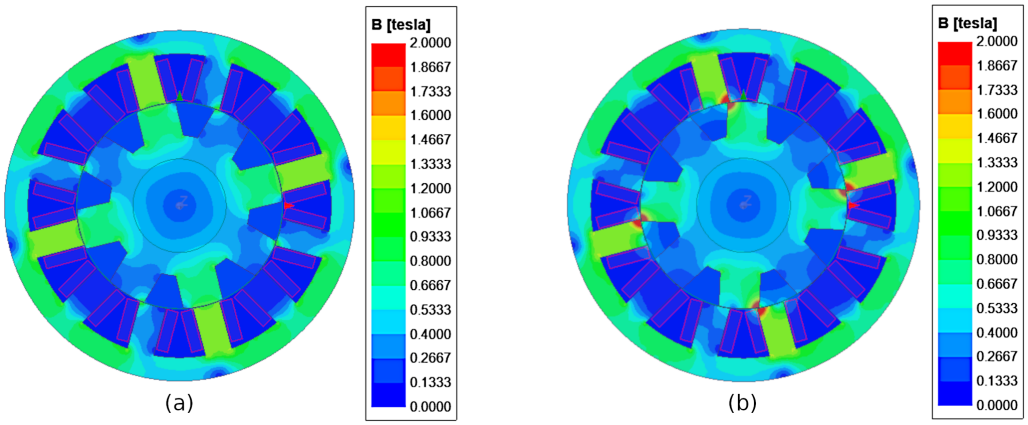

Figure 4. Magnetic flux distribution of conventional SRM: (**a**) aligned poles and (**b**) unaligned poles.

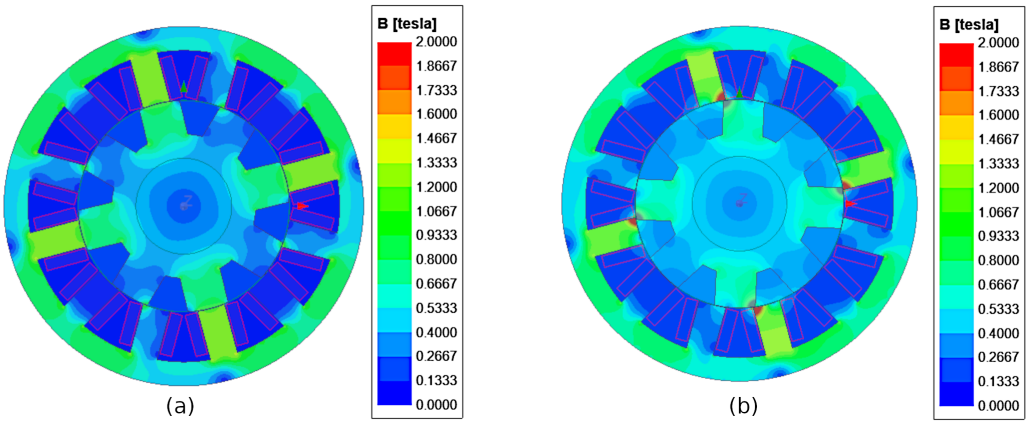

Figure 5. Magnetic flux distribution of HESRM: (**a**) aligned poles and (**b**) unaligned poles.

The reluctance principle governs SRM. Therefore, the SRM generates the torque based on the magnetic reluctance of the motor. The magnetic circuit between the rotor and stator is very reluctant when they are not in alignment. As the rotor tries to align with the powered stator poles at this point, the stator pole pairs are activated, reducing the magnetic reluctance. Reluctance torque is formed when the rotor is able to reach the minimal point of reluctance. It is necessary to precisely time the stator poles' excitation so that it only happens when the rotor is attempting to align with the exciting pole. SRM may require positive feedback from encoders or Hall effect sensors in order to control the excitation of the stator based on a precise rotor position.

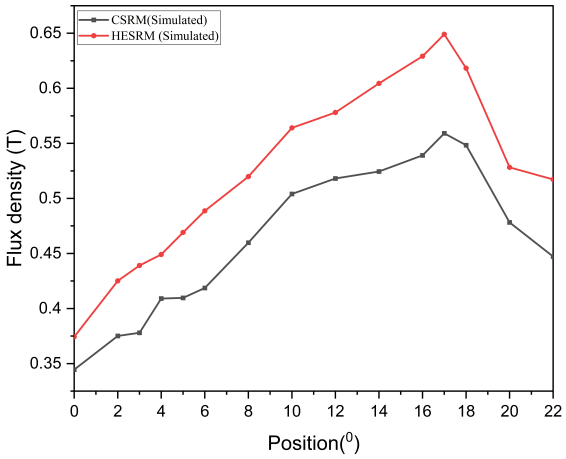

Figure 6. Simulated flux density of conventional SRM and the hybrid DC-excited SRM.

3.2. Steady-State Characteristics

The electromagnetic behaviour of the proposed HESRM was analyzed through the FEM (finite element method) using commercial software ANSYS/Maxwell. The motor drive simulation was carried out by MATLAB/Simulink, and the interpretation was held by the co-simulation method. For this purpose, the feasibility of the proof of concept was verified with the help of software simulations by analyzing steady-state and dynamic behaviors.

Static Electromagnetic Torque

The static magnetic torque characteristics of two SRMs with phase excitations are shown in Figure 7. The conventional SRM static torque curves with the current of 15 A vary from 0 to 22.5 degrees, as shown in Figure 7a. Accordingly, the static torque for one-half of the excitation cycle of conventional SRM attains unalignment to the aligned pole. It can be seen that the torque varies from minimum to maximum and finally reaches a minimum with the unaligned position. The maximum static torque that produces the phase excitation current of 15 A is 2 N m. From the comparison, it is clear that the auxiliary excitation in which a different current is provided with the help of DC injection may attain different patterns of static currents. The auxiliary winding has a provision for carrying the maximum current to the rated value. Figure 7b shows that the static flux curve pattern increases the effect of varying according to the rises of DC in the auxiliary coils. Since additional current is passed through DC injection in auxiliary windings using special circuitry, the flux inside the core increases, which results in higher torque and power density.

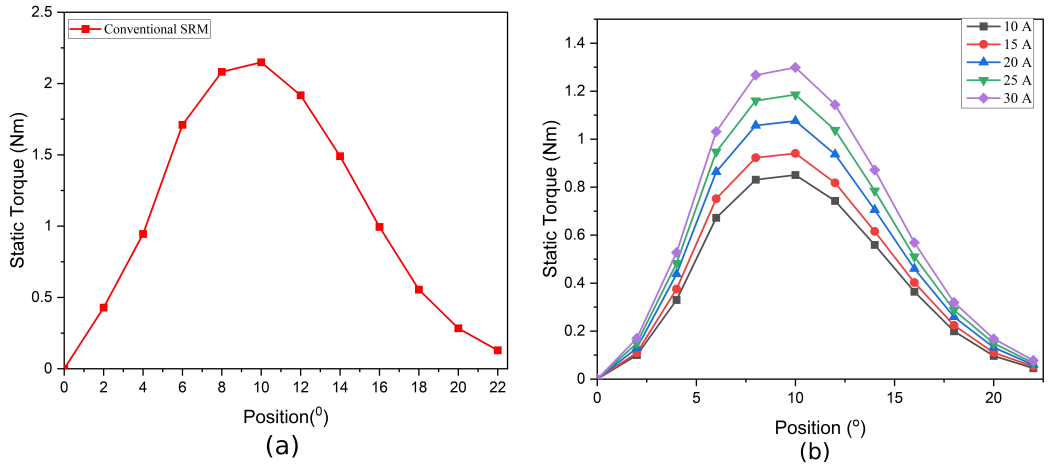

Figure 7. Static torque characteristics: (**a**) conventional SRM at rated current 15 A. (**b**) HESRM under various currents with respect to the DC field injection.

3.3. Dynamic Performance of Two SRM Drives

MATLAB/Simulink was used to study the performance of the motor drive system for two SRMs. The proposed HESRM drive system's Simulink model has an asymmetric half-bridge converter, logic PWM, angle controller mechanical systems, DC sources, speed and current controllers, a separate auxiliary excitation with an extra switch, etc. The machine model is developed on the Ansys/Maxwell workbench. The dynamic performance of both machines was performed and compared under the same conditions.

3.3.1. Gate Pulse Characteristics of Two SRMs

Figure 8 shows the moving torque and current characteristics of two SRMs in which the gate pulses are given to the phases at the same turn ON and turn OFF times. In conventional SRM, the single PWM pulses sequentially provide the switching scheme for all phases. The hybrid excitation method provides identical gate pulses to the main and auxiliary windings separately. The torque characteristics of conventional SRM can be achieved with similar excitations in HESRM. Since the moving torque remains similar, the auxiliary current can be further increased to the rated value to achieve maximum performance.

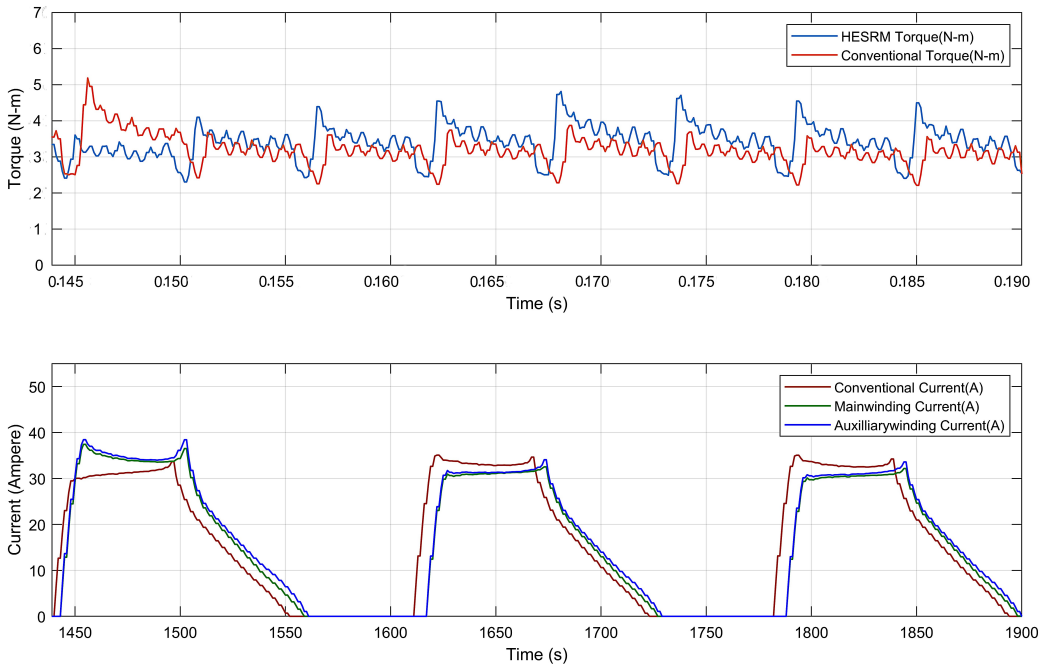

Figure 8. Comparison of characteristics of moving torque and current of two SRMs.

3.3.2. Closed-Loop Current Control of Two SRMs

The closed-loop current control of the conventional SRM is established by obtaining current feedback from the windings and providing input to the current controller. The conventional and proposed HESRM showed similar results at various input currents with matching moving torque and slightly less ripple, as shown in Figure 9. The current from the windings can be sensed and used to provide additional flux through the auxiliary in this hybrid excitation method.

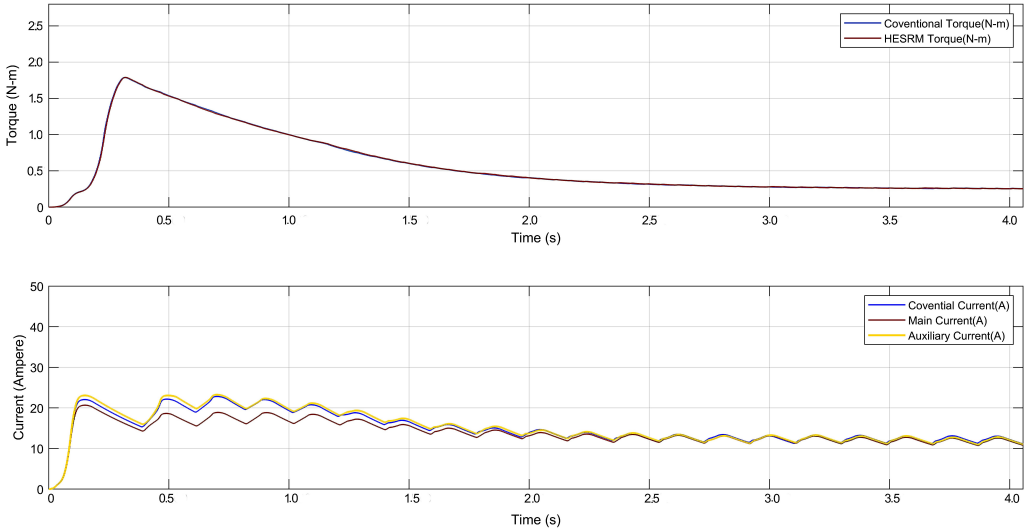

Figure 9. Comparison of closed-loop current control of conventional SRMs and HESRM.

3.3.3. Variable-Speed Control Strategy for Two SRMs

In Figure 10, the speed control is established using a proportional–integral (PI) controller by measuring the actual speed and comparing it with the reference speed, which varies continuously from minimum to rated value. The proportional (k_p) and integral (k_i) values of the controller are tuned in such a way as to reach the set points as early as possible. The analysis of the two results shows similar characteristics at the same current rating and load. The additional torque needed for the motor can be identified and provided through these auxiliary windings to obtain better results. However, the HESRM method is derived to enhance the performance by separately injecting the DC with the help of auxiliary winding. Hence, these results elaborate on how to achieve the same performance through the different winding excitations separately. However, the HESRM makes it possible only through different currents passing through the assigned winding. This method benefits by changing different currents through the controller to improve the average torque characteristics and reduce the torque ripple to the minimum level.

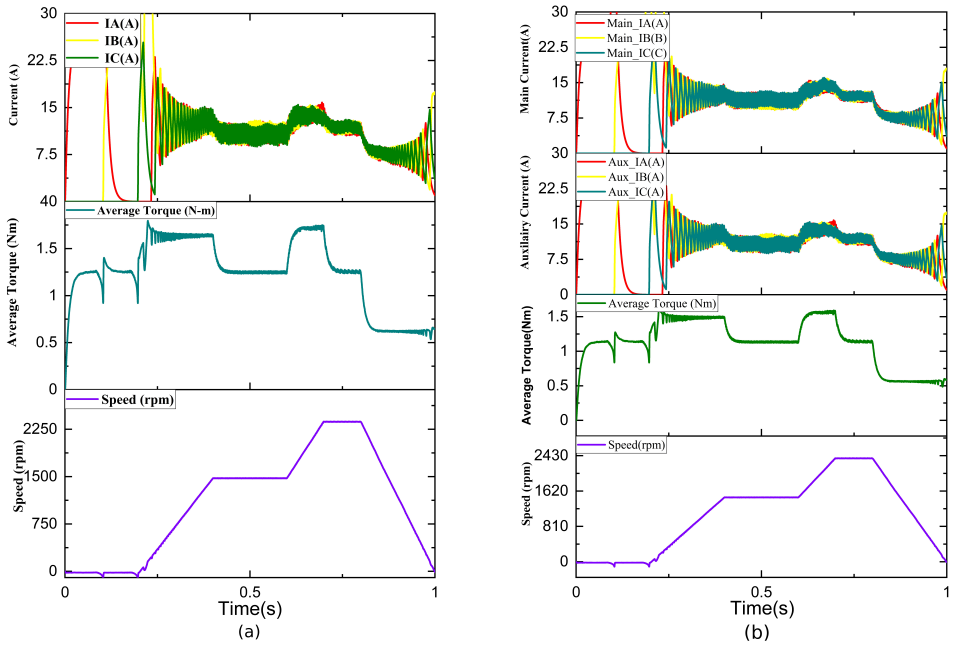

Figure 10. Closed-loop variable-speed current control strategy: (**a**) conventional SRM and (**b**) HESRM; the curves are current (A), torque (N-m), and speed (rpm).

In a conventional SRM, the variable speed is related to the main current excitation and torque, whereas in a HESRM, where there are two currents—the main current and an auxiliary current—the main current is responsible for both the excitations, and the auxiliary speed current is responsible for the variable speed. Figure 10 displays the torque and current characteristics of the traditional and hybrid SRM at variable speeds. To simulate how EVs would operate in real time, the speed input is changed using ramps and steps. Steps of 1000 rpm are used to ramp up the speed from zero to 2500 rpm. The graphs show all three phases of the currents at various speeds. Since this motor is a three-phase switching machine, the irregularities in the phase currents are caused by the speed changes. The motor's transient behavior is indicated by the longer switching patterns at the start of the operation.

4. Experimental Results

4.1. Motor Prototype

The torque characteristic of the SRM is the most important performance parameter that must be measured. As shown in Figure 11, in order to analyze the characteristics, a back-to-back motor setup with a torque sensor coupled in between was constructed. The motor used on the load side is a Permanent Magnet Synchronous Machine (PMSM) rated at 5000 revolutions per minute (rpm). This motor is tightly coupled with the motor of the plant. The non-linearity of the Futek torque sensor (model: TRD605) is +/−0.2%. This high-precision strain gauge sensor measures up to 250 N-m. The load-side PMSM contains an incremental speed encoder with a pulse per revolution (PPR) of 1024, which can be increased to 5000 by counting the rising and falling edges of the encoder's pulses. The PMSM's back EMF is used to drive a three-phase rectifier to a resistive load. Changes to the resistance can be made to load the motor.

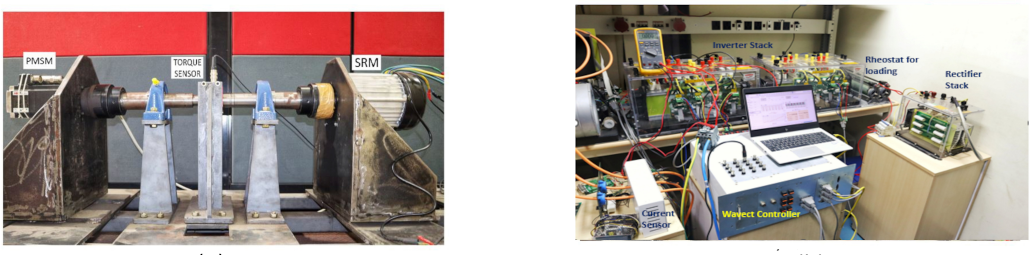

Figure 11. (**a**) Experimental setup of static measurements and (**b**) controller test setup of the proposed HESRM.

4.2. Dynamic Performance of HESRM without PMs

The dynamic performance of the conventional SRM and the proposed HESRM can be analyzed by enabling a closed-loop model. The experimental setup for both SRM drives is identical in all aspects and conditions. For the analysis, conventional drive systems are used, while in the auxiliary, additional circuits provide excitation. The motor has three hall sensors that are electrically separated by one degree. Using an asymmetric inverter stack, the three phases can be changed to run the motor. The control mechanism was enabled using Wavect, a universal rapid control prototyping platform for Motor Control Drives developed by Entuple Technologies, India. This FPGA-based controller implementation was developed to analyze real-time strategies that can be modeled, tested, and managed. The current sensors in the "wavect controller" can obtain the instantaneous phase currents, and torque can be compared via an ADC channel in the controller. The primary advantage of this mechanism is the ability to compare current and torque simultaneously. Figure 12 depicts the rewinding structure and the waveform corresponding to the obtained moving torque and peak current when the motor is tested at various speeds and loaded to its peak current.

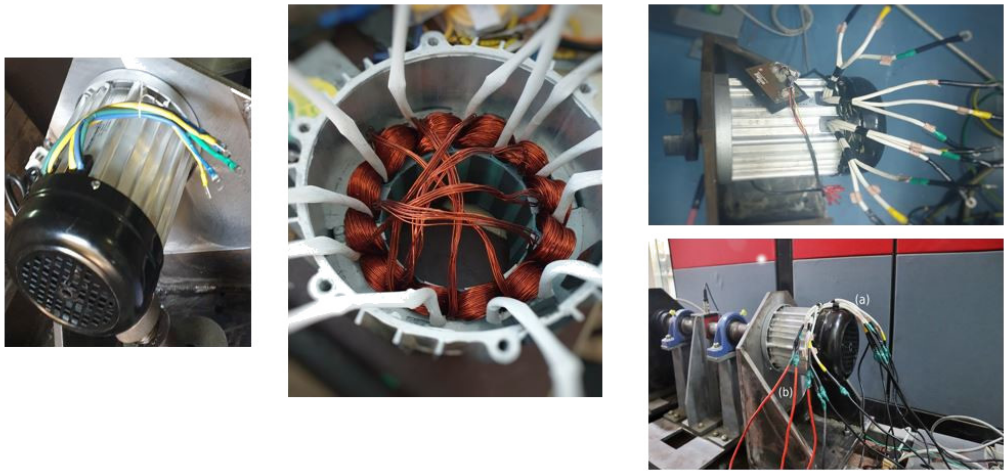

Figure 12. Photograph of rewinding the conventional SRM to HESRM (a) Main winding (b) Auxiliary winding.

Figure 13 depicts the conventional SRM phase current and torque performance at 1000 and 2000 rpm. Figure 14 depicts the analysis of the auxiliary current and torque for the hybrid excitation method. The three-phase current is denoted by different colours, and green indicates the auxiliary exciting current. In this method, both the primary and secondary poles are excited simultaneously without injecting any currents; the performance matches the Ansys/Matlab software simulation results.

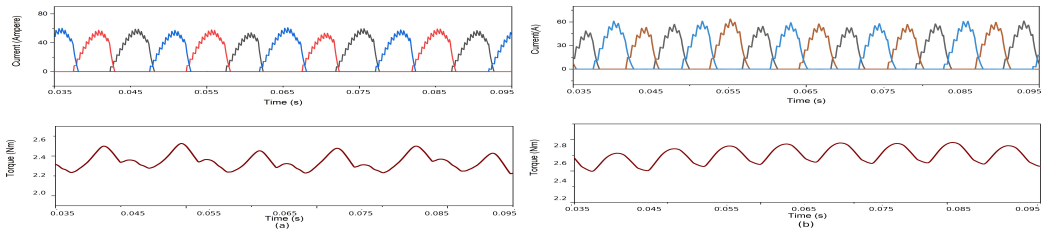

Figure 13. Conventional SRM dynamic performance of variable speed: (**a**) 1000 rpm and (**b**) 2500 rpm.

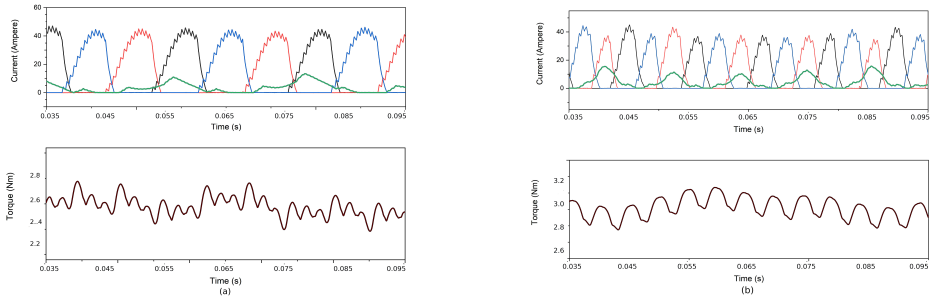

Figure 14. Proposed HESRM dynamic performance of variable speed: (**a**) 1000 rpm and (**b**) 2500 rpm.

The transient start-up response of the torque, phase current, and speed for two SRM drives with closed-loop control are tested and shown in Figure 15. The results under the same condition were evaluated with the DC-link voltage at 60 V and the load torque at 2 N m, respectively. It was found that both SRMs perform start-up in a similar way, according to the switching scheme provided, and accelerate rapidly as per the commanded speed of 1000 rpm to rated 2500 rpm. They reach the time of 50 ms and 500 ms, respectively. In other words, the speed changes from 500 rpm to 2500 rpm under closed-loop control, and the gain parameter changes in a real-time manner to reach the commanded speed. The result shows the rotor speed tracks the command signal in all manner and achieves the substantial results obtained from the simulated one.

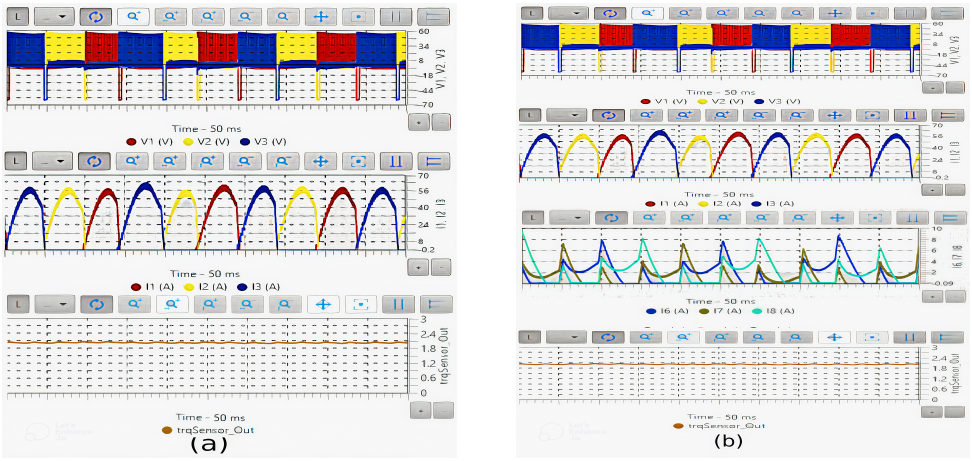

Figure 15. Closed-loop transient response at reference speed: (**a**) conventional SRM and (**b**) HESRM.

Figure 16 depicts the comparison between the measured and simulated average torque characteristics. The graphical analysis shows that the measured and simulated torque values are nearly identical. The average torque increased between 1000 and 2500 revolutions per minute. In Figure 16a, at an initial speed of 1000 rpm, the average torque begins at 1.8 N m. It increases exponentially as the effect of the auxiliary current varies. Variable-speed motors are permitted to adjust the auxiliary current from minimum to maximum, up to the rated value. Therefore, there is a tendency to provide more flux, thereby increasing the probability that the electromagnetic torque in the active region will increase.

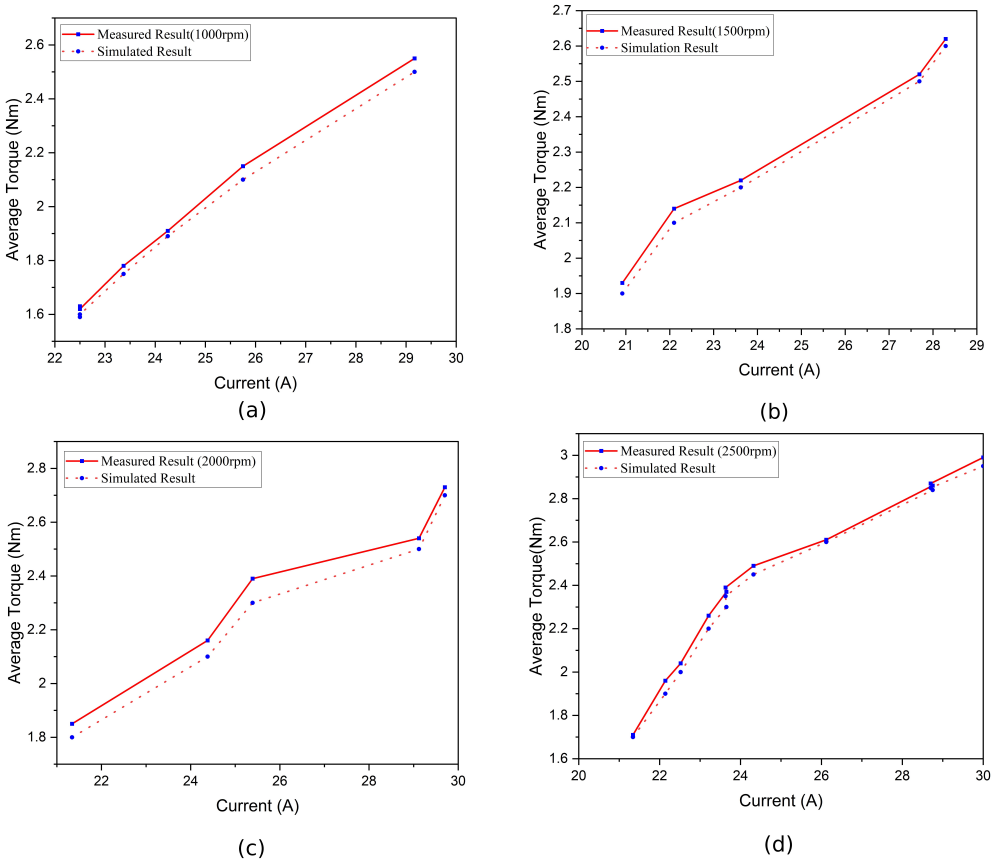

Figure 16. Average torque performance for variable speed of proposed HESRM: (**a**) 1000, (**b**) 1500, (**c**) 2000, and (**d**) 2500.

5. Comparison of Hardware Solution with FEM Simulation Results

In order to validate the proof of concept with results from the software analysis and theoretical perdition, a 12/8 conventional SRM and a rewound SRM of the same size for the proposed method were prototyped and experimentally validated. The main dimensions and parameter specifications of the two SRMs are shown in Table 1.

Figure 17 depicts the comparison of the average torque between the conventional SRM and the proposed HESRM at various speeds. To demonstrate the benefit of this novel machine structure, the hybrid excitation without a permanent magnet is compared with two SRMs from the same platform. The average performances for the speed range vary from 1000 rpm to 2500 rpm, shown in different figures. At 1000 rpm, the torque is 2 N m with the conventional current and excitation, while it reaches 2.5 N m with the auxiliary. For this reason, there is a significant increase in torque performance, and the percentage of torque increase at all speeds is greater than 20%. The pattern of torque response increase varies depending on speed and load.

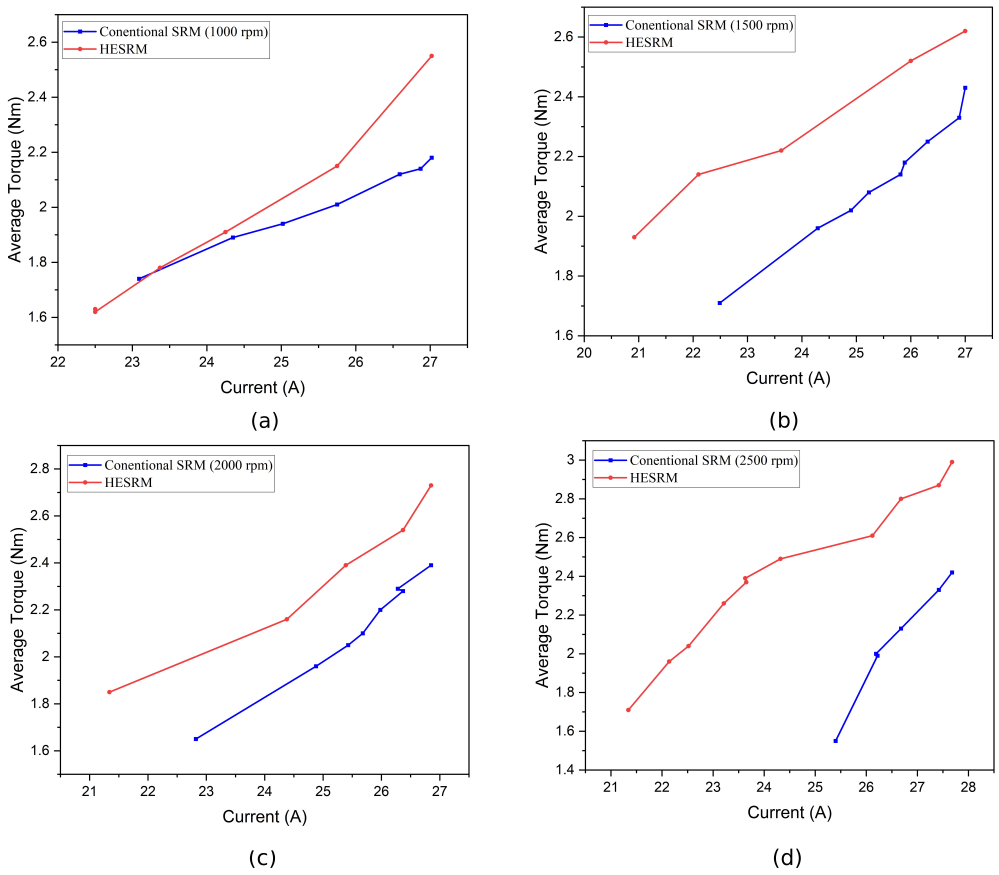

Figure 17. Comparison of average torque with variable speed for conventional SRM and proposed HESRM: (**a**) 1000, (**b**) 1500, (**c**) 2000, and (**d**) 2500 rpm.

6. Discussion

Figure 18a shows the plots of conventional and HESRM's average torque characteristics for various speeds. Both have a difference of 1 to 2 N m at 500 rpm, and it gradually increases. The HESRM reaches almost 2.4 N m at 1500 rpm, whereas the conventional one is only 2.1 N m. The HESRM reaches a maximum torque of 2.6 N m at 2500 rpm with a lead of almost 0.3 N m.

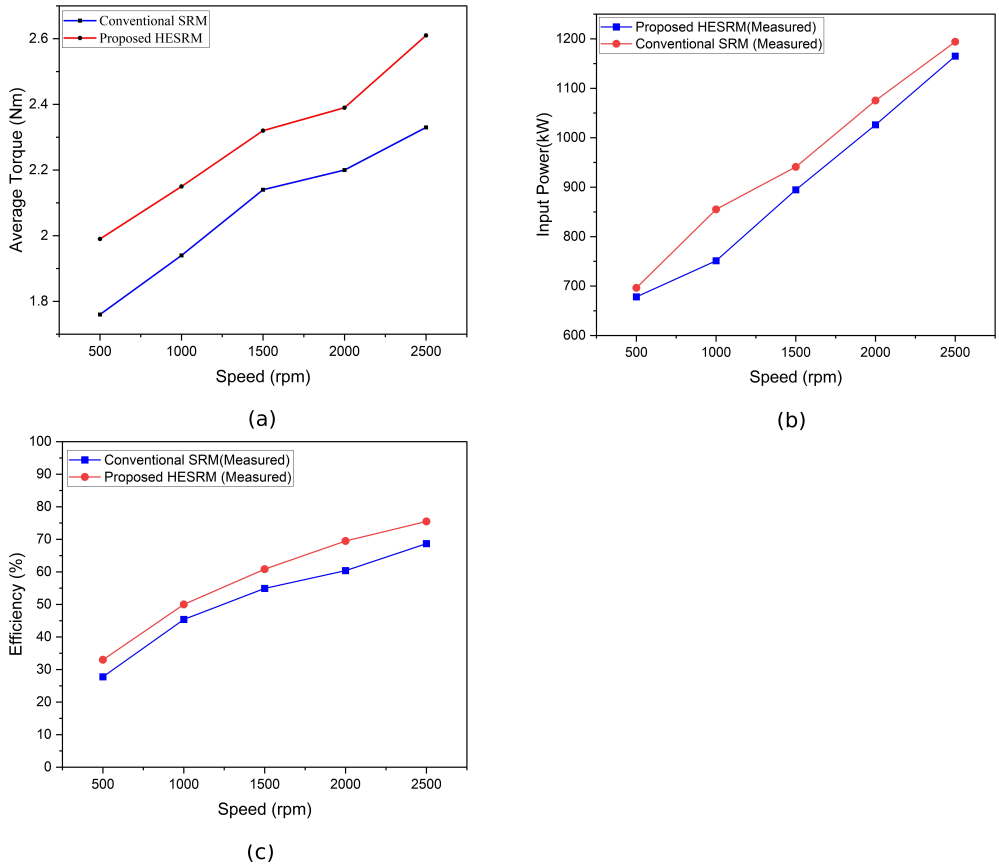

Figure 18. Comparison of conventional SRM with proposed HESRM: (**a**) average torque, (**b**) efficiency, and (**c**) input power.

The efficiencies for both SRMs were almost identical at the beginning of the test at 500 rpm. As speed increases, the efficiency of the HESRM makes clear leads compared with the conventional one. Up to 1500 rpm, the efficiencies of both motors follow a linear path with a difference of approximately 10%. At the rated speed of 2500 rpm, the efficiency of the motor differs to a maximum value of 80% and a minimum of 65%. The efficiency of the HESRM increased by 20%, as shown in Figure 18b.

The input power consumed by both motors is almost constant at 500 rpm, as clearly seen in Figure 18c. As the speed increases, the input power consumed by the motors starts to increase. The conventional SRM intakes more power at all the respective rpm compared with the proposed one. At 1000 rpm, the conventional SRM draws almost 850 W, whereas the HESRM draws a minimum of 700 W. At maximum speed, the input power consumed has a difference of almost 50 W.

Torque ripple is one of the major drawbacks of SRM, and thereby the hybrid excitation methods tend to provide higher possibilities. The proposed new HESRM without PM tends to exhibit less torque ripple than the conventional HESRM. In contrast, the conventional SRM exhibits a ripple of 3.72% at 2500 rpm, which decreases to 3.69% at 2000 rpm. Simultaneously, the proposed HESRM reduces torque ripple as a result of reduced pole switching, achieving 1.44% and 1.69% at 2500 and 2000 rpm, respectively.

7. Conclusions

When the average, static, and speed–torque characteristics of conventional and DC-injected hybrid SRMs are compared, it was found that significant improvements were made by HESRM over conventional SRM. In addition, the properties and performance of the machines are improved without sacrificing their fundamental qualities. In addition to a high torque-per-ampere rating, it offers high efficiency, high dependability, and redundancy.

The standard SRM is outperformed by the proposed method, and it generates greater torque at significantly lower current levels. Furthermore, the proposed HESRM employs separate excitations for the windings, thereby enhancing the versatility of the controller.

The proposed topology may be a replacement for HESRM machines with PM insertion. Since this study clearly demonstrates enhanced performance, the proposed system can be implemented in a variety of applications, such as electric vehicles. Moreover, improved average and smooth speed–torque characteristics have been achieved, which can be an excellent solution for EVs. Finally, this new topology can achieve greater efficiency with reduced torque ripple. Future objectives of this research include the design and implementation of advanced, optimized controllers to further reduce torque ripples. We are planning to study variable-speed control strategies for SRMs along with new designs.

Author Contributions: Conceptualization, V.A.; formal analysis, V.A. and M.J.H.; investigation, V.A. and P.A.S.; writing—original draft preparation, V.A.; writing—review and editing, M.J.H. and G.L.; supervision, M.J.H. and G.L.; industrial support, S.V.R. and T.P.M., concept analysis M.J.H. and S.V.R.; experimental analysis, V.A. and P.A.S. All authors have read and agreed to the published version of the manuscript.

Funding: The research is funded by the "University of Technology, Sydney".

Data Availability Statement: Not applicable.

Acknowledgments: I would like to acknowledge "Entuple Technologies" for providing the universal controller 'Wavect 300' and "Entuple E Mobility", Bangalore, India, for supporting the entire hardware implementation and testing setup during this work.

Conflicts of Interest: The authors declare no conflict of interest.

Abbreviations

The following abbreviations are used in this manuscript:

SRM	Switched Reluctance Motor
HESRM	Hybrid Excitation of Switched Reluctance Motors
PM	Permanent Magnet
EVs	Electric Vehicles
BLDCMs	Brushless DC Machines
ICE	Internal Combustion Engine
FEM	Finite Element Analysis

References

1. Lan, Y.; Benomar, Y.; Deepak, K.; Aksoz, A.; Baghdadi, M.E. Switched Reluctance Motors and Drive Systems for Electric Vehicle Powertrains: State of the Art Analysis andFuture Trends. *Energies* **2021**, *14*, 2079. [CrossRef]
2. Xu, J.; Zhang, L.; Meng, D.; Su, H. Simulation, Verification and Optimization Design of Electromagnetic Vibration and Noise of Permanent Magnet Synchronous Motor for Vehicle. *Energies* **2022**, *15*, 5808. [CrossRef]
3. Men, X.; Guo, Y.; Wu, G.; Chen, S.; Shi, C. Implementation of an Improved Motor Control for Electric Vehicles. *Energies* **2022**, *15*, 4833. [CrossRef]
4. Martellucci, L.; Capata, R. High Performance Hybrid Vehicle Concept—Preliminary Study and Vehicle Packaging. *Energies* **2022**, *15*, 4025. [CrossRef]
5. Tomczewski, K.; Wrobel, K.; Rataj, D.; Trzmiel, G. A Switched Reluctance Motor Drive Controller Based on an FPGA Device with a Complex PID Regulator. *Energies* **2021**, *14*, 1423. [CrossRef]
6. Rahman, M.S.; Lukman, G.F.; Hieu, P.T.; Jeong, K.; Ahn, J. Optimization and Characteristics Analysis of High Torque Density 12/8 Switched Reluctance Motor Using Metaheuristic Gray Wolf Optimization Algorithm. *Energies* **2021**, *14*, 2013. [CrossRef]
7. Pupadubsin, R.; Kachapornkul, S.; Jitkreeyarn, P.; Somsiri, P.; Tungpimolrut, K. Investigation of Torque Performance and Flux Reversal Reduction of a Three-Phase 12/8 Switched Reluctance Motor Based on Winding Arrangement. *Energies* **2022**, *15*, 284. [CrossRef]
8. Wang, J.; Jiang, W.; Wang, S.; Lu, J.; Williams, B.W.; Wang, Q. A Novel Step Current Excitation Control Method to Reduce the Torque Ripple of Outer-Rotor Switched Reluctance Motors. *Energies* **2022**, *15*, 2852. [CrossRef]
9. Kocan, S.; Rafajdus, P.; Bastovansky, R.; Lenhard, R.; Stano, M. Design and Optimization of a High-Speed Switched Reluctance Motor. *Energies* **2021**, *14*, 6733. [CrossRef]

10. Ding, W.; Member; Liu, G.; Li, P. A hybrid control strategy of hybrid-excitation switched reluctance motor for torque ripple reduction and constant power extension. *IEEE Trans. Ind. Electron.* **2020**, *67*, 38–48. [CrossRef]
11. Kabir, M.A.; Husain, I. Design of Mutually Coupled Switched Reluctance Motors (MCSRMs) for Extended Speed Applications Using 3-Phase Standard Inverters. *IEEE Trans. Energy Convers.* **2016**, *31*, 436–445. [CrossRef]
12. Elmutalab, M.A.; Elrayyah, A.; Husain, T.; Sozer, Y. Extending the Speed Range of a Switched Reluctance Motor Using a Fast Demagnetizing Technique. *IEEE Trans. Ind. Appl.* **2018**, *54*, 3294–3304. [CrossRef]
13. Lee, C.; Krishnan, R.; Lobo, N.S. Novel Two-Phase Switched Reluctance Machine Using Common-Pole E-Core Structure: Concept, Analysis, and Experimental Verification. *IEEE Trans. Ind. Appl.* **2009**, *45*, 703–711. [CrossRef]
14. Mecrow, B.C.; El-Kharashi, E.A.; Finch, J.W.; Jack, A.G. Segmental rotor switched reluctance motors with single-tooth windings. *IEE-Electr. Power Appl.* **2003**, *150*, 591–599. [CrossRef]
15. Mecrow, B.C.; El-Kharashi, E.A.; Finch, J.W.; Jack, A.G. Preliminary Performance Evaluation of Switched Reluctance Motors With Segmental Rotors. *IEEE Trans. Energy Convers.* **2004**, *19*, 679–686. [CrossRef]
16. R, V.; Fernandes, B.G. Design Methodology for High-Performance Segmented Rotor Switched Reluctance Motors. *IEEE Trans. Energy Convers.* **2015**, *30*, 11–21. [CrossRef]
17. Ding, W.; Yang, S.; Hu, Y.; Li, S.; Wang, T.; Yin, Z. Design Consideration and Evaluation of a 12/8 High-Torque Modular-Stator Hybrid Excitation Switched Reluctance Machine for EV Applications. *IEEE Trans. Ind. Electron.* **2017**, *64*, 9221–9232. [CrossRef]
18. Ding, W.; Fu, H.; Hu, Y. Characteristics Assessment and Comparative Study of a Segmented-Stator Permanent-Magnet Hybrid-Excitation SRM Drive With High-Torque Capability. *IEEE Trans. Power Electron.* **2018**, *33*, 482–500. [CrossRef]
19. Hasegawa, Y.; Nakamura, K.; Ichinokura, O. A Novel Switched Reluctance Motor With the Auxiliary Windings and Permanent Magnets. *IEEE Trans. Magn.* **2012**, *48*, 3855–3858. [CrossRef]
20. Zhihui, C.; Yaping, S.; Yangguang, Y. Static Characteristics of a Novel Hybrid Excitation Doubly Salient Machine. In Proceedings of the International Conference on Electrical Machines and Systems (ICEMS), Nanjing, China, 27–29 September 2005. [CrossRef]
21. Sulaiman, E.; Kosaka, T.; Matsui, N. High Power Density Design of 6-Slot–8-Pole Hybrid Excitation Flux Switching Machine for Hybrid Electric Vehicles. *IEEE Trans. Magn.* **2011**, *47*, 4453–4456. [CrossRef]
22. Jia, S.; Qu, R.; Li, J.; Li, D.; Kong, W. A Stator-PM Consequent-Pole Vernier Machine With Hybrid Excitation and DC-Biased Sinusoidal Current. *IEEE Trans. Magn.* **2017**, *53*, 1–4. [CrossRef]
23. Ahn, J.-W.; Park, S.-J.; Lee, D.-H. Hybrid Excitation of SRM for Reduction of Vibration and Acoustic Noise. *IEEE Trans. Ind. Electron.* **2004**, *51*, 374–380. [CrossRef]
24. Lu, K.; Jakobsen, U.; Rasmussen, P.O. Single-Phase Hybrid Switched Reluctance Motor for Low-Power Low-Cost Applications. *IEEE Trans. Magn.* **2011**, *47*, 3288–3291. [CrossRef]
25. Lu, K.; Rasmussen, P.O.; Watkins, S.J.; Blaabjerg, F. A New Low-Cost Hybrid Switched Reluctance Motor for Adjustable-Speed Pump Applications. *IEEE Trans. Ind. Appl.* **2011**, *47*, 314–321. [CrossRef]
26. Lu, K.Y.; Rasmussen, P.O.; Watkins, S.J.; Blaabjerg, F. A New Low-Cost Hybrid Switched Reluctance Motor for Adjustable-Speed Pump Applications. In Proceedings of the 2006 IEEE Industry Applications Conference Forty-First IAS Annual Meeting, Tampa, FL, USA, 8–12 October 2006. [CrossRef]
27. Nakamura, K.; Ichinokura, O. Super-MultipolarPermanent Magnet Reluctance Generator Designed for Small-Scale Wind-Turbine Generation. *IEEE Trans. Magn.* **2012**, *48*, 3311–3314. [CrossRef]
28. Nakamura, K.; Ichinokura, O. Super-Multipolar Permanent Magnet Reluctance Generator Designed for Small-Scale Renewable Energy Generation. In Proceedings of the International Conference on Electrical Machines, ICEM, Marseille, France, 2–5 September 2012. [CrossRef]
29. Lee, C.; Krishnan, R. New Designs of a Two-Phase E-Core Switched Reluctance Machine by Optimizing the Magnetic Structure for a Specific Application: Concept, Design, and Analysis. *IEEE Trans. Ind. Appl.* **2009**, *45*, 1804–1814. [CrossRef]
30. Abhijith, V.; Hossain, M.J.; Lei, G.; A S, P. Performance Improvement of Switched Reluctance Motor Using Hybrid Excitation Method Without Permanent Magnets. In Proceedings of the 2021 24th International Conference on Electrical Machines and Systems (ICEMS), Gyeongju, Korea, 31 October–3 November 2021.